THE JOURNAL OF BIOLOGICAL CHEMISTRY VOL. 287, NO. 5, pp. 3019–3028, January 27, 2012

p21 Cooperates with DDB2 Protein in Suppression of Ultraviolet Ray-induced Skin Malignancies*[S]

Received for publication, August 19, 2011, and in revised form, December 9, 2011 Published, JBC Papers in Press, December 13, 2011, DOI 10.1074/jbc.M111.295816

Tanya Stoyanova[‡1,2], Nilotpal Roy[‡1,3], Shaumick Bhattacharjee[‡], Dragana Kopanja[‡], Ted Valli[§], Srilata Bagchi[¶4], and Pradip Raychaudhuri[‡5]

From the [‡]Department of Biochemistry and Molecular Genetics, Cancer Center, University of Illinois at Chicago, Chicago, Illinois 60607, [§]VDx Pathology, Davis, California 95616, and the [¶]Center of Molecular Biology of Oral Diseases, College of Dentistry, Cancer Center, University of Illinois at Chicago, Chicago, Illinois 60612

Background: The p53-induced genes *DDB2* and *p21* play antagonistic roles in DNA repair and apoptosis.
Results: In UV-induced skin carcinoma, *DDB2* and *p21* cooperate to prevent carcinoma by inducing premature senescence.
Conclusion: Pro-senescence and anti-proliferative pathways are critical protection mechanism against skin malignancies.
Significance: Although studies on skin cancer focus on DNA repair mechanisms, this study provides new insights.

Exposure to ultraviolet rays (UV) in sunlight is the main cause of skin cancer. Here, we show that the p53-induced genes *DDB2* and *p21* are down-regulated in skin cancer, and in the mouse model they functionally cooperate to prevent UV-induced skin cancer. Our previous studies demonstrated an antagonistic role of DDB2 and p21 in nucleotide excision repair and apoptosis. Surprisingly, we find that the loss of *p21* restores nucleotide excision repair and apoptosis in *Ddb2*$^{-/-}$ mice, but it does not protect from UV-mediated skin carcinogenesis. In contrast, *Ddb2*$^{-/-}$*p21*$^{-/-}$ mice are significantly more susceptible to UV-induced skin cancer than the *Ddb2*$^{-/-}$ or the *p21*$^{-/-}$ mice. We provide evidence that *p21* deletion in the *Ddb2*$^{-/-}$ background causes a strong increase in cell proliferation. The increased proliferation in the *Ddb2*$^{-/-}$*p21*$^{-/-}$ background is related to a severe deficiency in UV-induced premature senescence. Also, the oncogenic pro-proliferation transcription factor FOXM1 is overexpressed in the *p21*$^{-/-}$ background. Our results show that the anti-proliferative and the pro-senescence pathways of DDB2 and p21 are critical protection mechanisms against skin malignancies.

The UV rays in sunlight cause DNA damage by generating cyclobutane pyrimidine dimers and 6-(1,2)-dihydro-2-oxo-4-pyrimidinyl-5-*methyl*-2,4-(1*H*,3*H*)-pyrimidinedione between two adjacent pyrimidines. Both DNA damages lead to distortion of DNA, predisposing cells to accumulate mutations. As a protective mechanism against UV-induced DNA damage, cells utilize nucleotide excision repair (NER)[6] pathway or they undergo apoptosis. Damaged DNA-binding protein 2 (DDB2), a subunit of the damaged DNA-binding protein DDB, encoded by the XP-E gene, plays important roles in both NER and apoptosis following exposure to UV irradiation (1–3). *Ddb2*$^{-/-}$ mice develop UV-induced skin cancers with much higher incidence in comparison with wild type (WT) mice (4, 5). Enhanced expression of *Ddb2* in mice also reduces UV-induced carcinogenesis by delaying the onset of tumor development and also by reducing the number of tumors per mouse, providing further evidence of the role of DDB2 in the inhibition of UV-induced skin tumorigenesis (6).

We demonstrated that high accumulation of p21 following exposure to low doses of UV light is the cause for the NER deficiency in the fibroblasts derived from the *Ddb2*-deficient embryos. DDB2 regulates the level of p21 through multiple mechanisms. DDB2 targets p53^{S18P} for proteolysis upon low dose of UV irradiation, ensuring lower expression of its downstream transcriptional target p21 (7). DDB2 also targets the p21 protein for proteolysis (8). p21 is not required for NER, as cells lacking p21 carry out NER efficiently following UV irradiation (9). We showed that deletion of *p21* in *Ddb2*-null background reverses the NER deficiency (7). Another study reported that *Gadd45*$^{-/-}$ keratinocytes accumulate p21 at a high level and that those keratinocytes are deficient in NER. Moreover, deletion of p21 restores NER capacity in *Gadd45*-deficient keratinocytes, further supporting the inhibitory role of p21 in NER (10).

The DDB2-deficient cells are resistant to UV-induced apoptosis (4, 8). We showed that upon treatment with DNA-damaging agents (cisplatin and aclarubicin) or high doses of UV light, accumulation of high levels of p21 in the *Ddb2*-deficient cells causes the apoptosis-deficient phenotype (8). Moreover, deletion of *p21* in the *Ddb2*-deficient background restores UV-

* This work was supported, in whole or in part, by National Institutes of Health Grants CA77637 and CA 156164 from NCI.
[S] This article contains supplemental Figs. S1 and S2.
[1] Both authors contributed equally to this work.
[2] Present address: Dept. of Microbiology, Immunology, and Molecular Genetics, University of California, 675 Charles E. Young Dr. S, Los Angeles, CA 90095.
[3] Supported by a Dean's Scholar Fellowship from the University of Illinois, College of Medicine.
[4] To whom correspondence may be addressed: College of Dentistry, Cancer Center, University of Illinois at Chicago, 801 S. Paulina Ave, Chicago, IL 60612. Tel.: 312-413-0683; E-mail: sbagchi@uic.edu.
[5] To whom correspondence may be addressed: Dept. of Biochemistry and Molecular Genetics (M/C 669), Cancer Center, University of Illinois at Chicago, 900 S. Ashland Ave., Chicago, IL 60607. Tel.: 312-413-0255; E-mail: pradip@uic.edu.

[6] The abbreviations used are: NER, nucleotide excision repair; MEF, mouse embryonic fibroblast; ROS, reactive oxygen species; DKO, double knockout; NL, normal; BCC, basal cell carcinoma; UDS, unscheduled DNA synthesis; TRITC, tetramethylrhodamine isothiocyanate; DCFDA, dichlorodihydrofluorescein diacetate; SA, senescence associated.

or DNA damage-induced apoptosis. Thus, after low doses of UV light, DDB2 ensures efficient repair, and when the DNA damage is too high to be repaired, DDB2 supports induction of apoptosis. Both processes involve attenuation of the levels of p21.

p21 is involved in senescence (11). Because DDB2 negatively regulates the levels of p21, we expected that the DDB2-deficient cells with high levels of p21 will undergo senescence prematurely. Contrary to that notion, the DDB2-deficient mouse embryonic fibroblasts (MEFs) are deficient in senescence and are prone to immortalization (12). Moreover, DDB2 expression in MEFs coincides with the onset of senescence (12). We demonstrated that DDB2 participates in inducing senescence through a completely different mechanism involving transcriptional repression of the antioxidant genes. In this study, we demonstrate that the premature senescence function of DDB2 plays a major role in suppressing UV-induced skin cancer, and p21 cooperates with DDB2 in the suppression.

MATERIALS AND METHODS

Mice—$p21^{-/-}$ mice were crossed with $Ddb2^{-/-}$ mice to produce $Ddb2^{+/-}p21^{+/-}$ progeny, which were crossed further to obtain the $Ddb2^{+/-}p21^{-/-}$ mice. The $Ddb2^{+/-}p21^{-/-}$ were crossed with $Ddb2^{+/-}p21^{-/-}$ to obtain $p21^{-/-}$ and $Ddb2^{-/-}p21^{-/-}$ mice. $Ddb2^{+/-}$ mice were crossed with $Ddb2^{+/-}$ mice to obtain $Ddb2^{-/-}$ and wild type mice.

Irradiation of Mice—10 to 15 mice each genotype were subjected to UV-B irradiation. Irradiation was carried out with FB-UVXL1000 UV cross-linker (Fisher) with UV-B tubes. Mice were exposed to UV light for 42 weeks, starting with 2 kJ/m^2 twice a week. The dose of UV light was gradually increased to 6 kJ/m^2 five times per week. Mice were shaved once a week. The dorsal area of the mice was exposed to UV-B.

BrdU Incorporation Assay—Mice were injected intraperitoneally at 100 μg of BrdU/g of body weight 4 h prior sacrificing. Skin sections were fixed, and immunostaining was performed with BrdU monoclonal antibody.

MEFs were pulse-labeled with 3 μg/ml BrdU for 1 h and 30 min and fixed with ice-cold 70% ethanol. Cells were kept with Denaturing solution (2 M HCl, 0.5% Triton X-100) for 1 h followed by 10 min of incubation with Neutralization solution (0.1 M sodium borate). Cells were incubated with BrdU monoclonal antibody (Dako; 1:500 dilution) overnight at 4 °C. After rinsing with PBS, cells were incubated with TRITC-conjugated polyclonal rabbit anti-mouse antibody for 2 h at room temperature and counterstained with DAPI.

Generation of Keratinocytes—Newborn pups were sacrificed and placed on ice and then washed with 70% EtOH. Skin was cut and peeled away from the posterior to anterior part of the body. The skins were placed in 6-cm dishes, dermal side up and spread. The skins were rinsed three times with 1× PBS and further treated with Dispase II (Roche Applied Science, 295 825) for 1 h at 37 °C. Epidermis was separated from the dermis, and the epidermis was floated in 3 ml of trypsin and incubated for 15 min at room temperature. Stratum corneum was removed, and the remaining cells were passed through cell dissociation sieve with 60–70 mesh screen. Trypsin was neutralized with FBS. Cells were spun down for 3 min. The cell pellets were resuspended in KGM-2 medium (Combrex BulletKit without Ca^{2+}, CC-3108) supplied with 50 μM $CaCl_2$ and plated on mouse collagen type IV precoated plates (BD Biosciences, 354233).

Unscheduled DNA Synthesis (UDS) Assays—Keratinocytes were grown on coverslips and treated with 10 mCi of [^{3}H]thymidine for 1 h in serum-free medium to distinguish the S phase cells. Cells were subjected to UV irradiation (12 J/m^2) and maintained in medium containing [^{3}H]thymidine for 3 h in the absence of serum. The cells were incubated in medium containing unlabeled thymidine for an additional 30 min and then fixed with methanol/acetic acid (3:1 ratio). Coverslips were placed on glass slides (cells facing up). Cells were further treated with 5% trichloroacetic acid in 1× PBS three times for 15 min each, followed by rinsing two times with 70% ethanol and one time with 100% ethanol to dry the coverslips completely. Under dark conditions, the slides were incubated in prewarmed EM-1 emulsion (Amersham Biosciences). The slides were left in a near vertical position for 10 min to drain the excess emulsion, followed by sealing in a light-tight box with anhydrous gels and storing at 4 °C for 5–7 days. Under darkroom conditions, slides were developed as follows; after 5 min in developing solution (prewarmed working strength D-19 Kodak), the reaction was stopped by incubation for 30 s in stop solution (working strength Kodak stop bath) and fixed for 10 min (Working Strength Fixer, Kodak). After fixation, the slides were exposed to light and washed four times for 15 min each with distilled H_2O. Pictures of random nuclei were taken with a Nikon microscope at ×100. Grains per nucleus (corresponding to DNA repair synthesis) were counted with Axio-Vision program.

Immunohistochemistry—Skin tissues were fixed in 10% buffered formalin and paraffin-embedded. Serial sections of 5 μm thickness were de-paraffinized in xylene, followed by rehydration in 100, 95, and 70% ethanol. Sections were further treated for antigen retrieval with citrate buffer, pH 6.0, at 95 °C for 20 min. Blocking was performed using mouse on mouse blocking reagents following the manufacturer's protocol (Vector Laboratories BMK-2202). The sections were incubated with the mouse anti-BrdU antibody 1:200 dilution (DAKO M0744) overnight. Sections were washed three times with 1× PBS, incubated with anti-mouse AP (Vector Laboratories AP-2000), and further developed with Alkaline Phosphatase Substrate (Vector Laboratories SK-5300) following the manufacturer's protocol. Nuclei were counterstained with Nuclear Fast Red.

Tissue Microarray—Human tissue microarray of normal (NL) and basal cell carcinoma (BCC) samples were obtained from US Biomax (SK482 and SK484). Immunohistochemical assay was performed as described above with antibodies against p21 (BD Biosciences) or against DDB2 (Abcam). Tissues were counterstained with hematoxylin. Intensity of staining was blind-scored from 0 (no staining) to 4 (highest intensity of staining). Graphs represent the average intensity of staining and paired *t* test of BCC *versus* NL scores of intensity of the staining.

Immunofluorescence—Skin tissues were fixed in 10% buffered formalin, and paraffin-embedded. Serial sections of 5 μm thickness were de-paraffinized in xylene, followed by re-hydration in 100, 95, and 70% ethanol. Sections were further treated

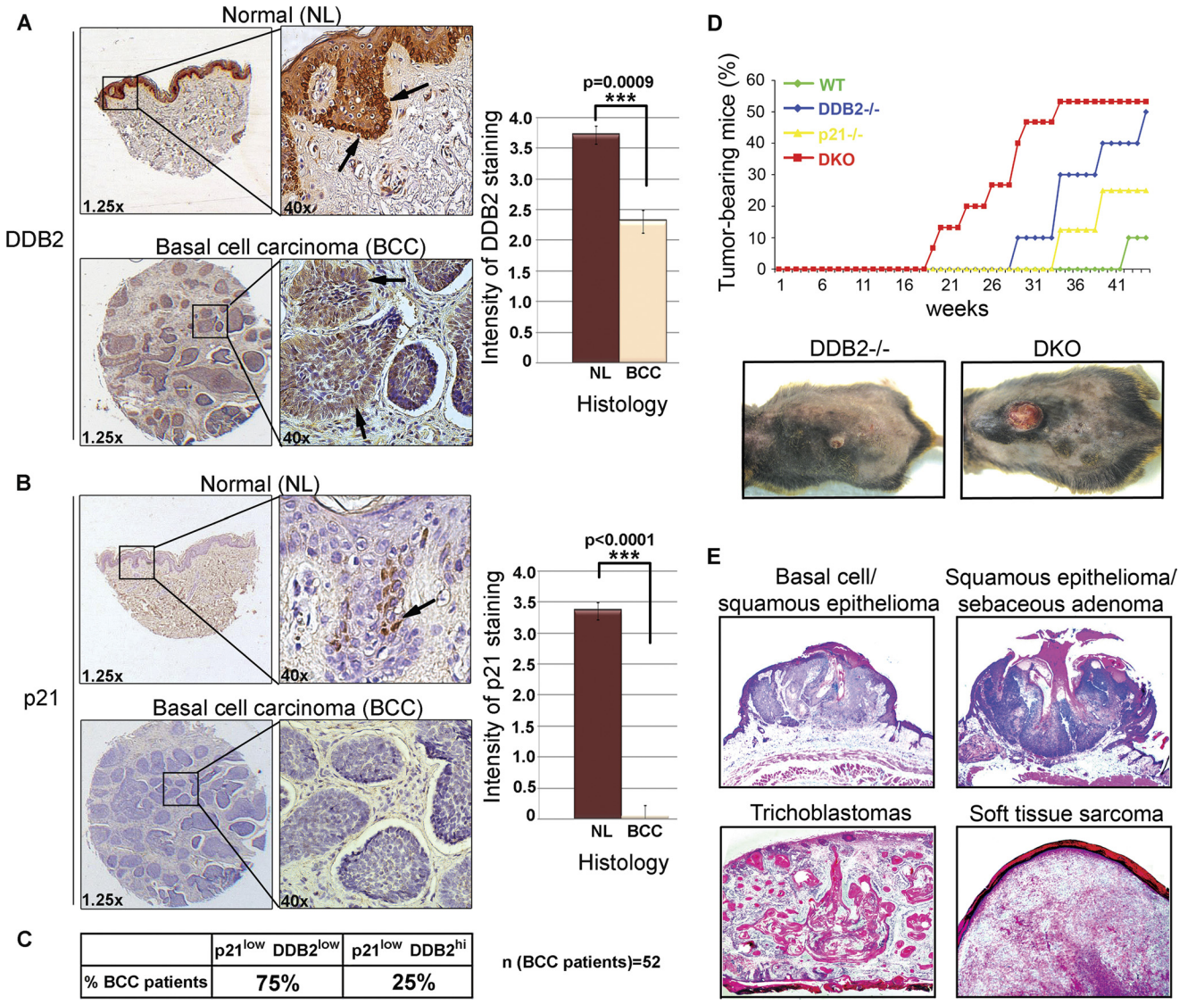

FIGURE 1. **Reduced expression of DDB2 and p21 in basal cell carcinoma, a synergistic increase in UV skin cancer in *Ddb2*$^{-/-}$*p21*$^{-/-}$ mice.** *A*, DDB2 immunohistochemistry of human tissue microarray of NL skin (*upper panel*) and BCC (*bottom panel*). Intensity of DDB2 staining was scored from 0 to 4. One representative of normal human skin section with score 4 ($n = 11$) (*upper panel*) and one representative of basal cell carcinoma with score 2 ($n = 52$) (*bottom panel*) are shown. *Right graph* represents the average intensity of DDB2 staining and *t* test for BCC *versus* NL. *B*, *upper panels* present p21 immunohistochemistry of human tissue microarray of NL skin ($n = 11$) with score 4, and the *bottom panels* present BCC ($n = 52$) with score 0. Intensity of p21 staining was scored from 0 to 4. *Right graph* presents the average intensity of p21 staining and *t* test for BCC *versus* NL. The *asterisks* in *A* and *B* indicate statistically significant differences. The *p* values were calculated by Student's *t* test (*A*, ***, $p < 0.0009$; *B*, ***, $p < 0.0001$). *C*, *table* presents percent basal cell carcinoma patients with lower p21 and DDB2 intensity of the staining in comparison with the average normal intensity of staining ($p21^{low}DDB2^{low}$). $p21^{low}DDB2^{hi}$ represents patients with lower than average normal p21 staining and equal to average normal DDB2 staining. *D*, wild type, *Ddb2*$^{-/-}$, *p21*$^{-/-}$, and DKO (*Ddb2*$^{-/-}$*p21*$^{-/-}$) mice at 8–12 weeks of age were chronically UV-irradiated for 42 weeks. Mice were shaved once a week, and the dorsal area was exposed to UV-B. Representative pictures of tumor-bearing *Ddb2*$^{-/-}$ and DKO (*bottom panels*) are shown. *E*, histological analysis of UV-induced tumors in the DKO (*Ddb2*$^{-/-}$*p21*$^{-/-}$) mouse is shown. ×2.5 magnification.

for antigen retrieval with citrate buffer, pH 6.0, at 95 °C for 20 min. Blocking was performed using 5% goat serum in PBS for 1 h at room temperature. Sections were incubated overnight at 4 °C using the following primary antibodies: p19Arf (5C3 Mab) and p16INK4a (SC-1207). After washing with PBS, sections were incubated with anti-rat or anti-rabbit immunoglobulin conjugated with FITC or TRITC. Coverslips were mounted in Vectashield (Vector Laboratories) containing DAPI to stain nuclei.

SA-β-Galactosidase Assay—Frozen skin sections were fixed in 3% formaldehyde in 1× PBS for 5 min at room temperature. Sections were washed two times with 1× PBS, pH 7.2, with 1 mM $MgCl_2$ and further incubated with X-gal staining solution overnight at 37 °C. Nuclei were counterstained with Nuclear Fast Red. Pictures of random fields were taken with Nikon microscope at ×10. SA-β-galactosidase-positive cells per field were counted.

MEFs were washed twice with ice-cold PBS. Cells were fixed with 2% formaldehyde and 0.2% glutaraldehyde solution in PBS. Cells were incubated at 37 °C overnight in staining solution containing 1 mg/ml X-gal, 40 mM citric acid/sodium phosphate, pH 6.0, 5 mM potassium ferrocyanide, 5 mM potassium ferricyanide, 150 mM NaCl, and 2 mM $MgCl_2$. Pictures of random fields were taken with Nikon microscope at ×100. SA-β-galactosidase-positive cells per field were counted.

Western Blot—Keratinocytes and skin tissue extracts were prepared in 0.4 M NaCl, 20 mM Tris-HCl, pH 7.5, 0.1% Nonidet P-40, 5% (v/v) glycerol, 1 mM sodium orthovanadate, and protease inhibitor mixture. Extracts (50–100 μg) were subjected to 10% SDS-PAGE followed by blotting to nitrocellulose membrane. The blots were probed with cdk2 (Santa Cruz Biotechnology), FoxM1 (Santa Cruz Biotechnology), catalase (Calbiochem), and $p21^{Waf1/Cip1}$ (BD Biosciences).

TUNEL—Keratinocytes were grown on glass coverslips and treated with UV-B or UV-C. Twenty four hours after treatment, cells were fixed in 1% paraformaldehyde, pH 7.4. The ApopTag Red *in situ* apoptosis detection kit (S7165) was used following the manufacturer's protocol. Paraffin-embedded tumor-free skin tissues from chronically UV-B-irradiated mice were subjected to TUNEL using ApopTag Red *in situ* apoptosis detection kit (S7165) following the manufacturer's protocol.

Analysis of ROS Production—Harvested skin sections were embedded and frozen in OCT compound, and frozen sections were prepared. Sections were stained with 10 μM 5-(6)-chloromethyl-2-dichlorodihydrofluorescein diacetate (CM-H_2DCFDA) (Invitrogen) for 45 min at 37 °C. Images were taken using a fluorescent microscope at ×20 magnification. Three to five randomly selected areas were photographed with the same exposure time. The images were processed using the same fixed threshold in all samples by Photoshop software, and representative images are shown.

RESULTS

Deletion of p21 Accelerates UV-induced Skin Cancers in $Ddb2^{-/-}$ Background—The *Ddb2* gene is mutated in XP-E, and its expression is reduced in a variety of cancers (13). One study reported DDB2 as one of the top 5% underexpressed genes in head and neck squamous cell carcinoma (14). Using tissue microarrays, we observed a significant loss of the DDB2 protein expression in BCCs (Fig. 1*A*). DDB2 participates in tumor suppression in at least three ways as follows: promoting NER, supporting apoptosis, and inducing premature senescence after DNA damage (7, 8, 12, 15–19). It participates in NER and apoptosis by maintaining p21 at a low level that is optimum for efficient repair synthesis and apoptosis (7, 8). However, expression of the p21 protein also is reduced in BCCs (Fig. 1*B*). The tissue microarray in our experiment contained 52 BCC samples of which 75% exhibited lower expression for DDB1 and p21 (Fig. 1*C*). *Ddb2* and *p21* are p53-induced genes (20, 21). It is possible that the reduced expression is related to *p53* mutations; however, the *p53* status in those BCC samples in the microarray, obtained from US Biomax, was not characterized. But it is noteworthy that *p53* is mutated at a high frequency in BCC (22, 23).

Because deletion of *p21* restores repair function and UV-induced apoptosis in the $Ddb2^{-/-}$ cells (7, 8), we sought to investigate the effects of *p21* deletion on the susceptibility to UV-induced skin carcinogenesis in the $Ddb2^{-/-}$ mouse. Wild type ($n = 10$), $Ddb2^{-/-}$ ($n = 10$), $p21^{-/-}$ ($n = 8$), and DKO ($Ddb2^{-/-}p21^{-/-}$) ($n = 15$) littermate mice were subjected to UV-B carcinogenesis protocol. We did not use $p21^{+/-}$ in the $Ddb2^{-/-}$ background because in that background stabilization rather than synthesis is the dominant factor that regulates the

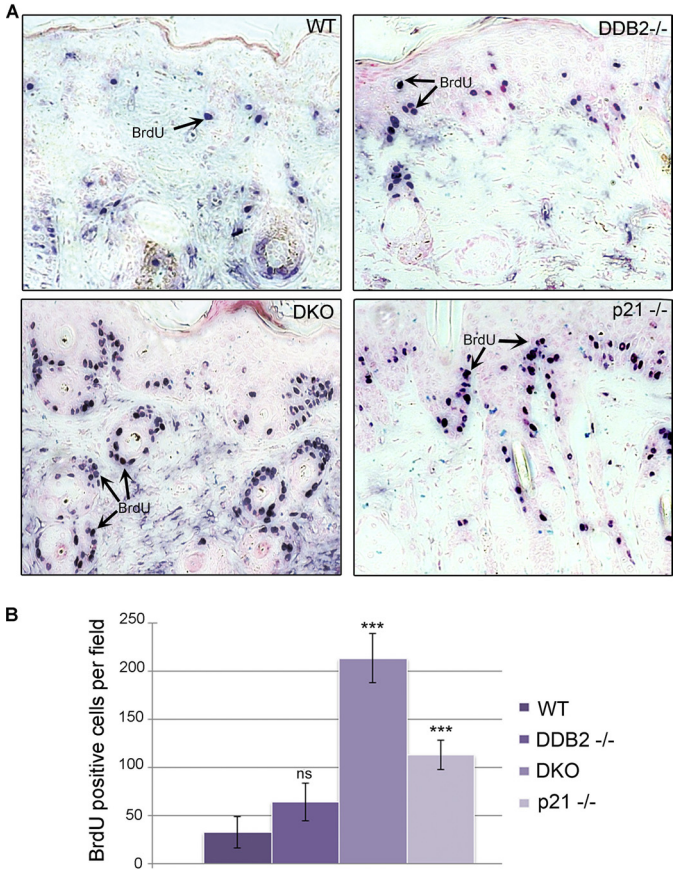

FIGURE 2. **Loss of *p21* in $Ddb2^{-/-}$ mice results in higher proliferation.** *A,* chronically UV-irradiated wild type, $Ddb2^{-/-}$, $p21^{-/-}$, and $Ddb2^{-/-}p21^{-/-}$ (*DKO*) mice were injected intraperitoneally with BrdU 4 h prior to sacrificing. Paraffin-embedded tissue was subjected to immunohistochemistry with BrdU antibody. *B,* BrdU-positive cells per ×10 magnification field were counted. Average of six different randomly chosen fields per mouse of each genotype is presented. The *asterisk* in *B* indicates statistically significant differences, with the following *p* value calculated by Student's *t* test: ***, $p < 0.001$; *ns,* not significant.

level of p21. There is a defect in p21 proteolysis in the $Ddb2^{-/-}$ background that causes accumulation of p21 after UV irradiation (8). Also, a previous study on skin carcinogenesis did not observe any significant difference in the $p21^{+/-}$ background compared with the $p21^{+/+}$ background (24). Also, the $Ddb2^{+/-}$ did not exhibit any significant deficiency in UV carcinogenesis experiments (5). The mice (the four genotypes indicated above) were shaved once a week and exposed to UV-B, initially 2 kJ/m2 twice a week for the first 8 weeks, followed by gradual increase of the frequency and dose of irradiation. The dose of UV-B used toward the end was 5 kJ/m2, five times per week. We observed that deletion of *p21* in the $Ddb2^{-/-}$ background did not reverse the susceptibility to UV-induced skin carcinogenesis (Fig. 1*D*). On the contrary, loss of *p21* in the $Ddb2^{-/-}$ background expedited the onset of tumor development. The $Ddb2^{-/-}p21^{-/-}$ mice developed tumors as early as 18 weeks post-UV treatment, and by 33 weeks 50% of the animals developed tumors. The $Ddb2^{-/-}$ mice started exhibiting tumor phenotypes at week 28, reaching 50% at week 42 (Fig. 1*D*). Only a few wild type mice exhibited papillary epithelioma beginning 41 weeks of treatment. The $p21^{-/-}$ mice exhibited increased susceptibility. All three genotypes ($p21^{-/-}$, $Ddb2^{-/-}$, and $p21^{-/-}Ddb2^{-/-}$)

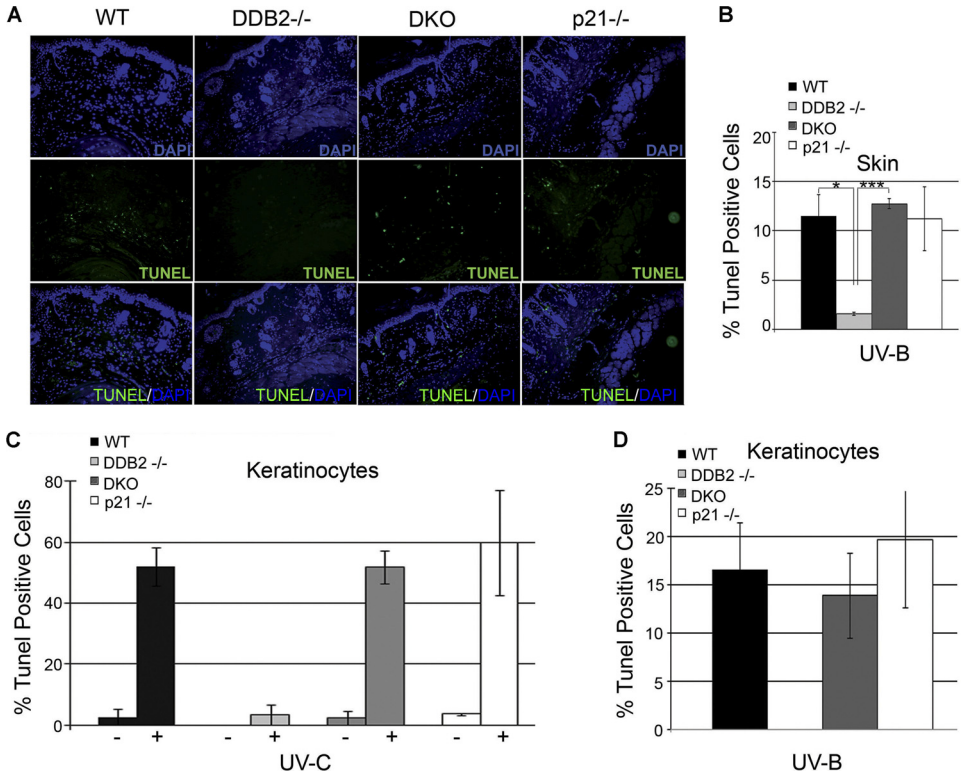

FIGURE 3. ***p21* deletion in *Ddb2*$^{-/-}$ background sensitizes mouse skin and keratinocytes to UV-induced apoptosis.** *A* and *B,* mice were chronically UV-irradiated for 30 weeks. Skin was isolated from tumor-free mice, wild type, *Ddb2*$^{-/-}$, *p21*$^{-/-}$, and *Ddb2*$^{-/-}$ *p21*$^{-/-}$ (DKO). Paraffin-embedded skin sections were subjected to TUNEL assay to measure apoptosis. Representative pictures are shown at ×10 magnification. The *asterisks* in *B* indicates statistically significant differences, with the following *p* value calculated by Student's *t* test: *, $p < 0.05$; ***, $p < 0.001$. *C* and *D,* keratinocytes were isolated from newborn pups, followed by UV irradiation. Eighteen hours post UV-C or UV-B exposure, apoptosis was measured by TUNEL.

developed basal cell carcinoma, squamous epithelioma, and soft tissue sarcomas (tumor sections from the *Ddb2*$^{-/-}$*p21*$^{-/-}$ are shown in Fig. 1*E*). Only the double knock-out mice exhibited trichoblastoma.

Strong Increase in Proliferation in the Ddb2$^{-/-}$*p21*$^{-/-}$ *Background*—The cyclin-dependent kinase inhibitor p21 functions as a major negative regulator of cell cycle progression. A recent study showed that the anti-proliferative activity of p21 is indispensable for inhibition of carcinogenesis upon chronic DNA damage to liver and kidneys (25). Therefore, we sought to investigate the extent of proliferation upon loss of *p21* in the *Ddb2*$^{-/-}$ mouse. We measured BrdU incorporation in the non-tumor skin sections from UV-irradiated mice from all four genotypes as follows: Wt, *Ddb2*$^{-/-}$, *p21*$^{-/-}$, and *Ddb2*$^{-/-}$*p21*$^{-/-}$. Tumor-bearing mice from the UV-induced carcinogenesis experiment (Fig. 1*D*) were injected intraperitoneally with BrdU 4 h before sacrificing. Immunohistochemical analysis revealed higher BrdU incorporation in the *Ddb2*$^{-/-}$*p21*$^{-/-}$ mouse skin in comparison with the WT, *Ddb2*$^{-/-}$, and *p21*$^{-/-}$ mouse skin (Fig. 2, *A* and *B*). The extent of BrdU incorporation in the double knock-out was significantly greater than the incorporations in each of the single knock-outs. The sections from the nontumor region were subjected also to TUNEL assay to determine the extent of apoptosis. As can be seen in Fig. 3, *A* and *B*, the sections from the *Ddb2*$^{-/-}$ mice were deficient in apoptosis, but no deficiency in apoptosis was observed in the double knock-out mice. This observation is consistent with our findings in MEFs (8). To further confirm the reversal of the UV-induced apoptosis in the keratinocytes, we measured the effect of *p21* deletion on apoptosis in keratinocytes upon exposure to UV-B and UV-C. Wild type, *Ddb2*$^{-/-}$, *p21*$^{-/-}$, or *Ddb2*$^{-/-}$ *p21*$^{-/-}$ keratinocytes were isolated from newborn pups and subjected to either UV-C (Fig. 3*C*) or UV-B (Fig. 3*D*). Apoptosis was measured by TUNEL assay. Consistent with our previous findings in MEFs and in the skin sections, the *Ddb2*$^{-/-}$ keratinocytes exhibited deficiency in apoptosis upon both UV-B and UV-C. Loss of *p21* in *Ddb2*$^{-/-}$ keratinocytes restored the sensitivity to apoptosis induced by UV damage. These observations suggest that the increased proliferation, but not the lack of apoptosis, in *Ddb2*$^{-/-}$*p21*$^{-/-}$ is responsible for accelerated tumor development.

Loss of p21 Restores the DNA Repair Synthesis in the Ddb2$^{-/-}$ *Keratinocytes*—Previously, we showed that in MEFs accumulation of p21 in the absence of DDB2 is due to higher expression and deficiency in degradation (7, 8). Moreover, deletion of *p21* reversed the repair-deficient phenotype of the *Ddb2*$^{-/-}$ MEFs (8). Consistent with the observations in the MEFs, we observed a significant increase in the level of p21 in the keratinocytes and in the skin from *Ddb2*$^{-/-}$ mice, both in the absence or presence of UV damage (Fig. 4, *A* and *B*). We measured NER DNA synthesis in keratinocytes in all four genotypes Wt, *Ddb2*$^{-/-}$, *p21*$^{-/-}$, and *Ddb2*$^{-/-}$*p21*$^{-/-}$ by assaying for unscheduled DNA synthesis (UDS) (Fig. 4*C*). UDS measures DNA synthesis in non-S phase cells induced by UV irradiation. Consistent with our earlier observation on MEFs, we found that *Ddb2*$^{-/-}$ keratinocytes exhibited deficiency in UDS, measured by grains per

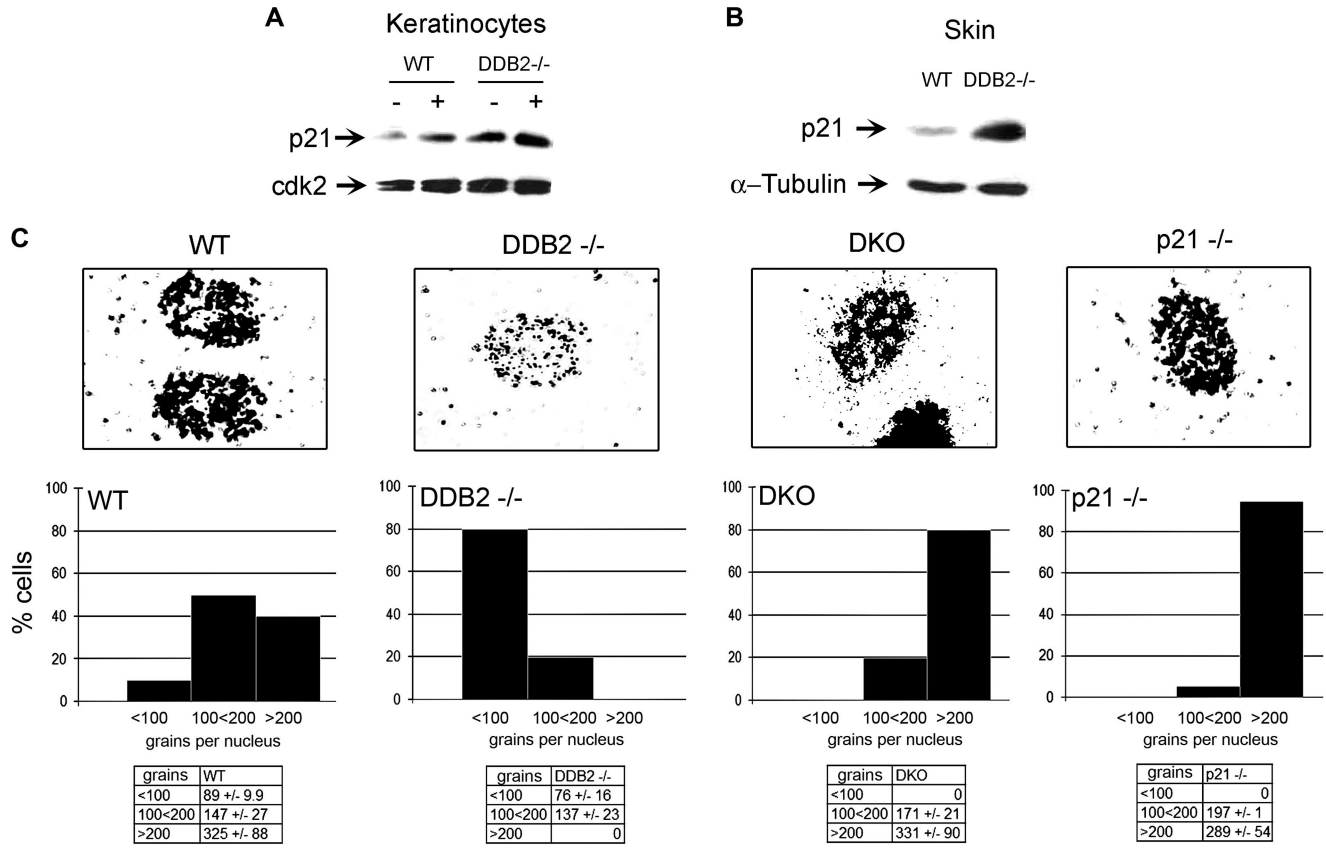

grains	WT
<100	89 +/- 9.9
100<200	147 +/- 27
>200	325 +/- 88

grains	DDB2 -/-
<100	76 +/- 16
100<200	137 +/- 23
>200	0

grains	DKO
<100	0
100<200	171 +/- 21
>200	331 +/- 90

grains	p21 -/-
<100	0
100<200	197 +/- 1
>200	289 +/- 54

FIGURE 4. **Loss of *p21* restores the DNA repair synthesis in *Ddb2*$^{-/-}$ keratinocytes.** *A, Ddb2*$^{-/-}$ keratinocytes have higher levels p21 in the absence and presence of UV-B. Extracts from wild type or *Ddb2*$^{-/-}$ keratinocytes either not treated or subjected to UV-B were subjected to Western blot analysis. *B,* extracts from wild type or *Ddb2*$^{-/-}$ mouse skin were subjected to Western blot analysis. *C,* keratinocytes from WT, *Ddb2*$^{-/-}$, *p21*$^{-/-}$, and *Ddb2*$^{-/-}$*p21*$^{-/-}$ were subjected to UDS analyses. Representative nuclei are shown (*upper panels*). After quantification, the numbers of grains per nucleus were plotted (*bottom panels*).

nucleus upon exposure to a single dose of UV-B (Fig. 4*C*). Deletion of *p21* in *Ddb2*$^{-/-}$ keratinocytes restored the UDS to levels comparable with that in the WT keratinocytes with most of the nuclei carrying over 200 grains per nucleus (Fig. 4*C*). Thus, the accelerated tumor development may not be related to the deficiency in repair synthesis in the double knock-out mice.

Ddb2$^{-/-}$*p21*$^{-/-}$ *Mice Are Severely Deficient in UV-induced Premature Senescence*—We previously demonstrated a role of DDB2 in cellular senescence (12). High level p21 has been suggested to play an important role in triggering senescence (26–29). Although *Ddb2*$^{-/-}$ cells have higher level of p21, these cells are deficient in premature senescence (12). We observed evidence that DDB2 and p21, in fact, have a synergistic effect in inducing premature senescence response following exposure to UV light. Mice of all four genotypes were exposed to acute UV-B followed by measurement of senescence response. We performed SA-β-galactosidase staining of skin sections from mice irradiated with UV-B (Fig. 5*A*) using a procedure described previously (30). Both *p21*$^{-/-}$ and *Ddb2*$^{-/-}$ mice exhibited deficiencies in senescence response in comparison with WT mice after UV damage (Fig. 5*A*). Interestingly, the *Ddb2*$^{-/-}$*p21*$^{-/-}$ mice exhibited a more severe deficiency in senescence response compared with the *Ddb2*$^{-/-}$ or the *p21*$^{-/-}$ mice (Fig. 5*A*). We confirmed the observation by assessing the level of *p16Ink4a* and *p19Arf*. Accumulation of *p19Arf* and *p16Ink4a* was observed in the WT mice and that was significantly reduced in the *p21*$^{-/-}$ and the *Ddb2*$^{-/-}$ mice (Fig. 5, *B* and *C,* and supplemental Fig. S1). Moreover, consistent with the SA-β-galactosidase staining, there was a near complete loss of *p19Arf* and *p16Ink4* expression in the *Ddb2*$^{-/-}$*p21*$^{-/-}$ mice, further confirming the notion that these mice are severely deficient in senescence, which might be the major contributing factor for the increased onset of tumorigenesis.

Instability of ROS and Increased Expression of FoxM1 in the Ddb2$^{-/-}$*p21*$^{-/-}$ *Mice*—Previously, we demonstrated that the senescence deficiency phenotype in *Ddb2*$^{-/-}$ mice is related to a deficiency in the accumulation of ROS. DDB2 supports ROS accumulation by repressing the antioxidant genes (12). ROS has been implicated also in the mechanism by which p21 participates in senescence (26). We measured the levels of ROS using DCFDA staining (detects peroxides) in the skin of all four genotypes following subacute UV irradiation. Cryosections of skin from WT, *Ddb2*$^{-/-}$, *p21*$^{-/-}$, and *Ddb2*$^{-/-}$*p21*$^{-/-}$ mice were treated with 10 μM DCFDA for 45 min at 37 °C and visualized under microscope (Fig. 6*A* and supplemental Fig. S2). Clearly, the *Ddb2*$^{-/-}$ and the *p21*$^{-/-}$ mice were deficient in peroxide accumulation compared with the WT mice. Moreover, the double knock-out skin sections also exhibited a stronger deficiency in peroxide accumulation (Fig. 6*A*). Extracts from the skin fragments of all four genotypes were compared by Western blot assays for catalase. Clearly, the skin extracts from the dou-

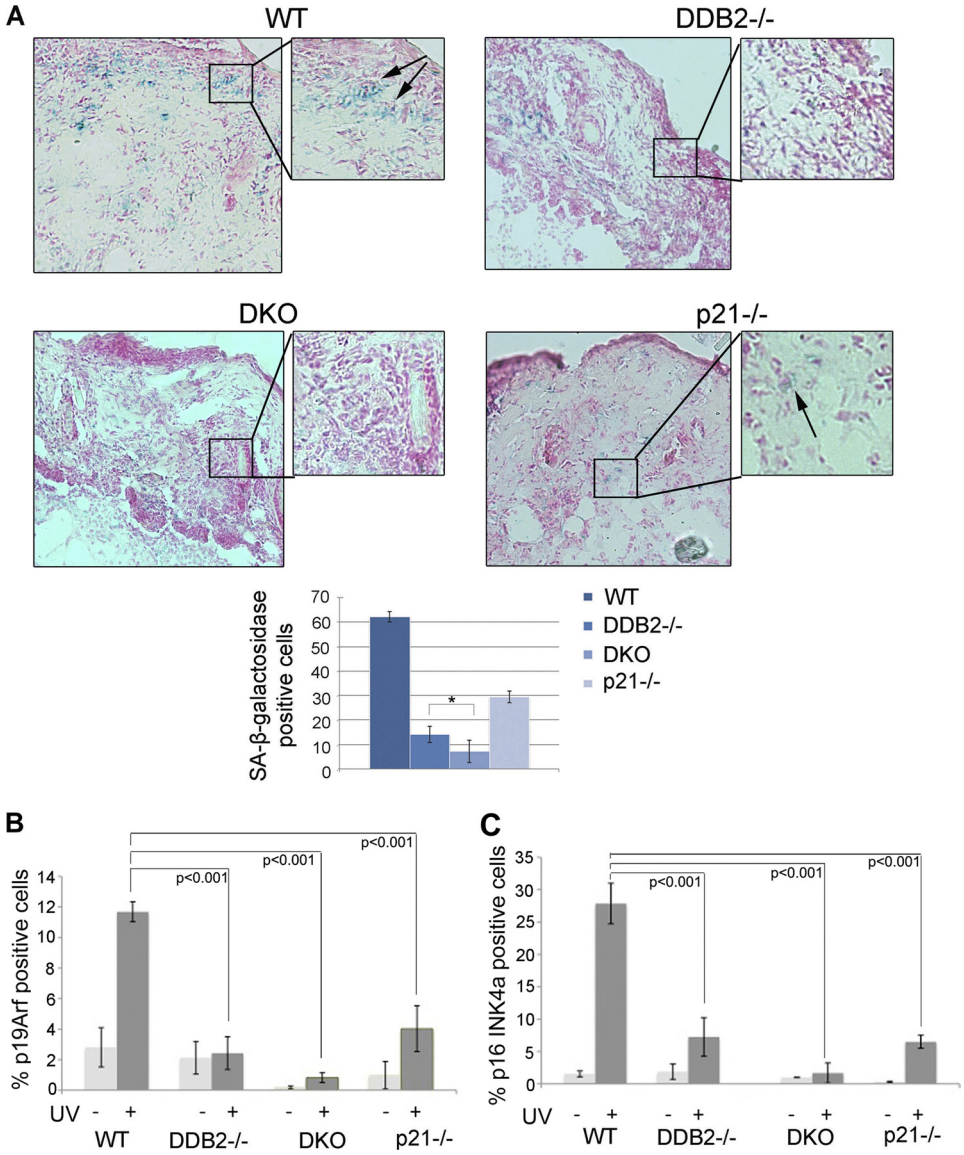

FIGURE 5. ***Ddb2*$^{-/-}$*p21*$^{-/-}$ mice are deficient in UV-induced senescence.** *A,* wild type, *Ddb2*$^{-/-}$, *p21*$^{-/-}$, and *Ddb2*$^{-/-}$*p21*$^{-/-}$ mice were irradiated with a single dose of UV radiation (10 kJ/m^2). Unfixed cryosections were prepared from the skin 24 h after UV radiation. Frozen skin sections were subjected to SA-β-galactosidase. *Arrows* indicate SA-β-galactosidase-positive cells. SA-β-galactosidase-positive cells per ×10 magnification field were counted. 10 random fields were chosen for quantification. *B* and *C,* wild type, *Ddb2*$^{-/-}$, *p21*$^{-/-}$, and *Ddb2*$^{-/-}$*p21*$^{-/-}$ mice were irradiated with a single dose of UV radiation (10 kJ/m^2). Mice were killed after 24 h, and their skin were fixed in 10% formalin, processed, and embedded with paraffin for sectioning. Prepared skin section slides were then subjected to immunocytochemical analysis using p16INK4A, p19ARF antibody, and DAPI. p16INK4A and p19ARF-positive staining identified senescent cells. p19ARF and p16INK4A-positive cells per ×10 magnification field were counted. 10 random fields were chosen for quantification.

ble knock-out mice exhibited a much higher expression of catalase (Fig. 6*B*). p21 has been implicated in regulating expression of *FoxM1* (31), a transcription factor that regulates oxidative stress-induced premature senescence and activates expression of proliferation genes, including genes involved in G_1 to S and G_2 to M progression (32, 33). Consistent with that, we observed a much higher expression of FOXM1 in the *p21*$^{-/-}$ background. Both *p21*$^{-/-}$ mice and the double knock-out mice expressed FOXM1 at much higher levels (Fig. 6*C*). The lack of senescence and increased expression of FOXM1 provide a clear explanation for the strong increase in proliferation in the *p21*$^{-/-}$*Ddb2*$^{-/-}$ mice. The higher rate of cell proliferation and reduced senescence after UV irradiation in the *p21*$^{-/-}$ *Ddb2*$^{-/-}$ background was confirmed also using MEFs (Fig. 6, *D* and *E*). It is noteworthy that the extent of increase in BrdU incorporation after UV irradiation in the double knock-out cells was somewhat less than what was seen in the *in vivo* experiment (Fig. 2*B*), which most likely reflects the differences in the *in vitro* and *in vivo* experimental set up. Finally, we observed that *N*-acetylcysteine, a ROS scavenger, inhibited UV-induced senescence (Fig. 6*F*), which is consistent with a role of ROS in inducing premature senescence following UV irradiation.

DISCUSSION

Results presented here are significant in several ways. First, although it is generally believed that DNA repair and apoptosis are important for preventing development of cancer cells, our results suggest a critical role of premature senescence in inhibiting UV-induced skin cancer. We show that premature senescence is more important than NER and apoptosis in inhibiting

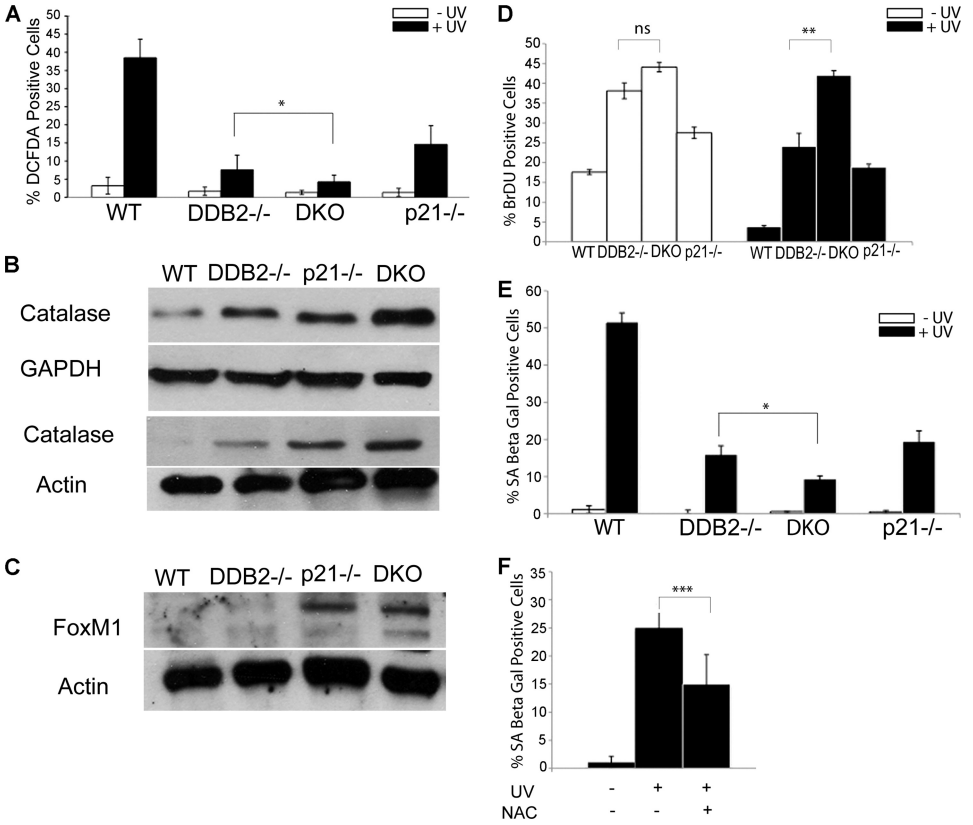

FIGURE 6. **Deficiency in UV-induced senescence in $Ddb2^{-/-}p21^{-/-}$ mice is due to low accumulation of ROS.** *A,* wild type, $Ddb2^{-/-}$, $p21^{-/-}$, and $Ddb2^{-/-}p21^{-/-}$ mice were irradiated with a single dose of UV light (10 kJ/m^2). Unfixed cryosections from treated and untreated mice were prepared from the skin 24 h after UV radiation. Cryosections were incubated with 10 μM DCFDA for 45 min at 37 °C to detect ROS. All images were photographed under ×20 magnification. ROS-positive cells per ×20 magnification field were counted. Average of six different randomly chosen fields per mouse of each genotype is presented. *B* and *C,* skin extracts from wild type, $Ddb2^{-/-}$, $p21^{-/-}$, and $Ddb2^{-/-}p21^{-/-}$ mice were subjected to Western blot analysis with catalase and FoxM1 antibody. Actin or GAPDH was used as loading control. Two different sets of mice have been shown for catalase expression. *D,* WT, $Ddb2^{-/-}$, $p21^{-/-}$, and $Ddb2^{-/-}p21^{-/-}$ MEFs were plated at equal density (1×10^5). Next day cells were treated with UV light (50 J/m^2). 48 h after UV treatment, BrdU (3 μg/ml) was added to the culture medium for 1 h and 30 min. The cells were fixed in 70% ice-cold ethanol and subjected to immunostaining for BrdU using monoclonal BrdU antibody. The cells were also stained with DAPI. The percent BrdU-positive cells from three experiments were plotted. *E,* WT, $Ddb2^{-/-}$, $p21^{-/-}$, and $Ddb2^{-/-}p21^{-/-}$ MEFs were plated at equal density (1×10^5). Next day cells were treated with UV light (50 J/m^2). 72 h after treatment cells were subjected to SA-β-galactosidase assay. SA-β-galactosidase assay-positive cells were counted from at least 10 fields of triplicate plates. *F,* WT MEFs were plated at equal density (1×10^5). Next day cells were treated with UV light (50 J/m^2) and kept with or without (*NAC*) (20 mM *N*-acetylcysteine). 72 h after treatment, cells were counted from at least 10 fields of triplicate plates. The *asterisk* in *A* and *D–F* indicates statistically significant differences, with the following *p* value calculated by Student's *t* test: *, $p < 0.05$; **, $p < 0.01$; ***, $p < 0.001$; *ns,* not significant.

UV-induced skin cancer. In addition, we show that the p53-induced genes *p21* and *Ddb2* play significant roles in that process. p21 and DDB2 cause accumulation of ROS to a high level following UV irradiation, leading to senescence.

UV skin carcinogenesis protocol involves irradiation of mice with high doses of UV-B, leading to extensive DNA damage that overwhelms the repair machinery. In the $Ddb2^{-/-}$ background the repair capacity becomes further limiting because of high levels of p21. The high level of p21 also inhibits apoptosis of the cells harboring irreparable DNA damages. Deletion of *p21* restored repair and apoptosis but did not restore premature senescence in $Ddb2^{-/-}$ mice. However, there was a stronger inhibition of premature senescence in the $Ddb2^{-/-}p21^{-/-}$ mice compared with the single knock-outs. In addition, there was a huge increase in proliferation in the skin of the UV-irradiated $Ddb2^{-/-}p21^{-/-}$ mice. We think that the increased proliferation and the lack of premature senescence of the UV-irradiated cells are responsible for acceleration of the tumor development in the $Ddb2^{-/-}p21^{-/-}$ mice. Our findings are consistent with a study demonstrating that $p21^{-/-}$ anti-proliferative function is indispensable for inhibition of tumorigenesis in the liver (25). Willenbring *et al.* (25) observed induction of p21 in $Fah^{-/-}$ mice, a mouse model of hereditary tyrosinemia type I, a human disorder characterized by accumulation of toxic metabolites that causes chronic DNA damage leading to hepatocellular carcinoma. $Fah^{-/-}$ hepatocytes also exhibit cell cycle arrest and deficiency in apoptosis (25). Apoptosis resistance in $Fah^{-/-}$ mice was found to be due to accumulation of p21, because its depletion restored apoptosis (25). Despite efficient apoptosis, deletion of *p21* in $Fah^{-/-}$ background resulted in rapid proliferation and cancer formation (25).

p21 inhibits cell proliferation and supports premature senescence through its ability to inhibit the CYCLIN-CDK kinases (34). The CYCLIN-CDK inhibitory function supports premature senescence by activation of the cell cycle inhibitory pathways of the retinoblastoma protein (34). The $Ddb2^{-/-}p21^{-/-}$ cells possess higher CYCLIN-CDK kinase activity (8), which is therefore expected to contribute to the lack of senescence in the double knock-out cells through inhibition of the retinoblastoma protein. Interestingly, consistent with a previous report

(26), we observed a role of p21 in the ROS accumulation, a mechanism that also contributes to senescence (35). In UV-irradiated skin, both *Ddb2*$^{-/-}$ and *p21*$^{-/-}$ mice accumulated much lower levels of ROS compared with that in the wild type mice. The levels of ROS in the double knock-outs were significantly lower than the levels observed in the single knock-outs, suggesting that p21 and DDB2 regulate ROS through distinct mechanisms. Consistent with that, there was a higher expression of catalase in the double knock-out skin samples compared with that in the single knock-outs. We showed that DDB2 functions as a repressor of the *Catalase* and *SOD2* genes (12). However, in the skin samples, MnSOD expression was not increased significantly in the absence of DDB2 (data not shown). It is likely that other mechanisms overcome the DDB2-mediated repression of MnSOD in skin. However, catalase expression was increased in the *Ddb2*$^{-/-}$ background. The increase was observed also in the *p21*$^{-/-}$ background, suggesting that p21 also represses *Catalase* expression. Interestingly, p21 was shown to repress expression of *FOXM1*, which is a proliferation-associated transcription factor that is also an activator of *Catalase* (31, 36). Interestingly, FOXM1 activates its own expression (37). But the activity of FOXM1 requires phosphorylation by CYCLIN-CDK (38). Therefore, it is possible that p21 inhibits FOXM1 expression by inhibiting its activation by the CYCLIN-CDK kinases. A reduced FOXM1 activity will reduce its own expression. Consistent with that, we observed a significantly higher expression of FOXM1 in the *p21*$^{-/-}$ background. High level of FOXM1 is known to inhibit premature senescence by attenuating oxidative stress or ROS (36). FOXM1 reduces oxidative stress by stimulating expression of several antioxidant genes, including *Catalase* (36).

The deficiency in premature senescence is expected to increase the proliferation, and therefore it could explain the high level proliferation in the *Ddb2*$^{-/-}$*p21*$^{-/-}$ background. The lack of p21 will increase CYCLIN-CDK activities, contributing to a higher rate of proliferation. In addition, the increased expression of FOXM1, a pro-proliferation transcription factor, is expected to contribute to proliferation significantly because it stimulates expression of SKP2 and CKS1 to promote G_1/S progression and stimulates a number of mitotic genes to promote G_2/M transition (32). Therefore, the high expression of FOXM1 in the *Ddb2*$^{-/-}$*p21*$^{-/-}$ background is expected to promote proliferation through activation of the cell cycle genes. FOXM1 is a target of the DNA damage checkpoint effectors, and its reduced expression has been implicated in the G_2/M delay following exposure to DNA-damaging agents (39). High expression of FOXM1 in the *p21*$^{-/-}$ background is expected to overcome the checkpoints in cells harboring irreparable DNA damage and therefore is expected to support accumulation of mutant cells. The *Ddb2*$^{-/-}$ cells to do not arrest after DNA damage (8). Therefore, the *Ddb2*$^{-/-}$*p21*$^{-/-}$ cells are expected to generate mutant cells at much higher rates, which is likely the basis for the acceleration of skin cancer development.

REFERENCES

1. Nichols, A. F., Itoh, T., Graham, J. A., Liu, W., Yamaizumi, M., and Linn, S. (2000) Human damage-specific DNA-binding protein p48. Characterization of XPE mutations and regulation following UV irradiation. *J. Biol. Chem.* **275,** 21422–21428
2. Tang, J., and Chu, G. (2002) Xeroderma pigmentosum complementation group E and UV-damaged DNA-binding protein. *DNA Repair* **1,** 601–616
3. Wittschieben, B. Ø., Iwai, S., and Wood, R. D. (2005) DDB1-DDB2 (xeroderma pigmentosum group E) protein complex recognizes a cyclobutane pyrimidine dimer, mismatches, apurinic/apyrimidinic sites, and compound lesions in DNA. *J. Biol. Chem.* **280,** 39982–39989
4. Itoh, T., Cado, D., Kamide, R., and Linn, S. (2004) DDB2 gene disruption leads to skin tumors and resistance to apoptosis after exposure to ultraviolet light but not a chemical carcinogen. *Proc. Natl. Acad. Sci. U.S.A.* **101,** 2052–2057
5. Yoon, T., Chakrabortty, A., Franks, R., Valli, T., Kiyokawa, H., and Raychaudhuri, P. (2005) Tumor-prone phenotype of the DDB2-deficient mice. *Oncogene* **24,** 469–478
6. Alekseev, S., Kool, H., Rebel, H., Fousteri, M., Moser, J., Backendorf, C., de Gruijl, F. R., Vrieling, H., and Mullenders, L. H. (2005) Enhanced DDB2 expression protects mice from carcinogenic effects of chronic UV-B irradiation. *Cancer Res.* **65,** 10298–10306
7. Stoyanova, T., Yoon, T., Kopanja, D., Mokyr, M. B., and Raychaudhuri, P. (2008) The xeroderma pigmentosum group E gene product DDB2 activates nucleotide excision repair by regulating the level of p21Waf1/Cip1. *Mol. Cell. Biol.* **28,** 177–187
8. Stoyanova, T., Roy, N., Kopanja, D., Bagchi, S., and Raychaudhuri, P. (2009) DDB2 decides cell fate following DNA damage. *Proc. Natl. Acad. Sci. U.S.A.* **106,** 10690–10695
9. Smith, M. L., Ford, J. M., Hollander, M. C., Bortnick, R. A., Amundson, S. A., Seo, Y. R., Deng, C. X., Hanawalt, P. C., and Fornace, A. J., Jr. (2000) p53-mediated DNA repair responses to UV radiation. Studies of mouse cells lacking p53, p21, and/or gadd45 genes. *Mol. Cell. Biol.* **20,** 3705–3714
10. Maeda, T., Espino, R. A., Chomey, E. G., Luong, L., Bano, A., Meakins, D., and Tron, V. A. (2005) Loss of p21WAF1/Cip1 in Gadd45-deficient keratinocytes restores DNA repair capacity. *Carcinogenesis* **26,** 1804–1810
11. Campisi, J., and d'Adda di Fagagna, F. (2007) Cellular senescence. When bad things happen to good cells. *Nat. Rev. Mol. Cell Biol.* **8,** 729–740
12. Roy, N., Stoyanova, T., Dominguez-Brauer, C., Park, H. J., Bagchi, S., and Raychaudhuri, P. (2010) DDB2, an essential mediator of premature senescence. *Mol. Cell. Biol.* **30,** 2681–2692
13. Oh, K. S., Emmert, S., Tamura, D., DiGiovanna, J. J., and Kraemer, K. H. (2011) Multiple skin cancers in adults with mutations in the XP-E (DDB2) DNA repair gene. *J. Invest. Dermatol.* **131,** 785–788
14. Bagchi, S., and Raychaudhuri, P. (2010) Damaged DNA-binding protein-2 drives apoptosis following DNA damage. *Cell Div.* **5,** 3
15. Kulaksiz, G., Reardon, J. T., and Sancar, A. (2005) Xeroderma pigmentosum complementation group E protein (XPE/DDB2). Purification of various complexes of XPE and analyses of their damaged DNA binding and putative DNA repair properties. *Mol. Cell. Biol.* **25,** 9784–9792
16. Reardon, J. T., and Sancar, A. (2003) Recognition and repair of the cyclobutane thymine dimer, a major cause of skin cancers, by the human excision nuclease. *Genes Dev.* **17,** 2539–2551
17. Wakasugi, M., Kawashima, A., Morioka, H., Linn, S., Sancar, A., Mori, T., Nikaido, O., and Matsunaga, T. (2002) DDB accumulates at DNA damage sites immediately after UV irradiation and directly stimulates nucleotide excision repair. *J. Biol. Chem.* **277,** 1637–1640
18. El-Mahdy, M. A., Zhu, Q., Wang, Q. E., Wani, G., Praetorius-Ibba, M., and Wani, A. A. (2006) Cullin 4A-mediated proteolysis of DDB2 protein at DNA damage sites regulates *in vivo* lesion recognition by XPC. *J. Biol. Chem.* **281,** 13404–13411
19. Sugasawa, K., Okuda, Y., Saijo, M., Nishi, R., Matsuda, N., Chu, G., Mori, T., Iwai, S., Tanaka, K., Tanaka, K., and Hanaoka, F. (2005) UV-induced ubiquitylation of XPC protein mediated by UV-DDB-ubiquitin ligase complex. *Cell* **121,** 387–400
20. Tan, T., and Chu, G. (2002) p53 Binds and activates the xeroderma pigmentosum DDB2 gene in humans but not mice. *Mol. Cell. Biol.* **22,** 3247–3254
21. el-Deiry, W. S., Tokino, T., Velculescu, V. E., Levy, D. B., Parsons, R., Trent, J. M., Lin, D., Mercer, W. E., Kinzler, K. W., and Vogelstein, B. (1993) WAF1, a potential mediator of p53 tumor suppression. *Cell* **75,** 817–825
22. Kim, M. Y., Park, H. J., Baek, S. C., Byun, D. G., and Houh, D. (2002)

Mutations of the p53 and PTCH gene in basal cell carcinomas. UV mutation signature and strand bias. *J. Dermatol. Sci.* **29,** 1–9
23. Shea, C. R., McNutt, N. S., Volkenandt, M., Lugo, J., Prioleau, P. G., and Albino, A. P. (1992) Overexpression of p53 protein in basal cell carcinomas of human skin. *Am. J. Pathol.* **141,** 25–29
24. Topley, G. I., Okuyama, R., Gonzales, J. G., Conti, C., and Dotto, G. P. (1999) p21(WAF1/Cip1) functions as a suppressor of malignant skin tumor formation and a determinant of keratinocyte stem-cell potential. *Proc. Natl. Acad. Sci. U.S.A.* **96,** 9089–9094
25. Willenbring, H., Sharma, A. D., Vogel, A., Lee, A. Y., Rothfuss, A., Wang, Z., Finegold, M., and Grompe, M. (2008) Loss of p21 permits carcinogenesis from chronically damaged liver and kidney epithelial cells despite unchecked apoptosis. *Cancer Cell* **14,** 59–67
26. Macip, S., Igarashi, M., Fang, L., Chen, A., Pan, Z. Q., Lee, S. W., and Aaronson, S. A. (2002) Inhibition of p21-mediated ROS accumulation can rescue p21-induced senescence. *EMBO J.* **21,** 2180–2188
27. Di Leonardo, A., Linke, S. P., Clarkin, K., and Wahl, G. M. (1994) DNA damage triggers a prolonged p53-dependent G_1 arrest and long term induction of Cip1 in normal human fibroblasts. *Genes Dev.* **8,** 2540–2551
28. Waldman, T., Kinzler, K. W., and Vogelstein, B. (1995) p21 is necessary for the p53-mediated G_1 arrest in human cancer cells. *Cancer Res.* **55,** 5187–5190
29. Bunz, F., Dutriaux, A., Lengauer, C., Waldman, T., Zhou, S., Brown, J. P., Sedivy, J. M., Kinzler, K. W., and Vogelstein, B. (1998) Requirement for p53 and p21 to sustain G_2 arrest after DNA damage. *Science* **282,** 1497–1501
30. Dimri, G. P., Lee, X., Basile, G., Acosta, M., Scott, G., Roskelley, C., Medrano, E. E., Linskens, M., Rubelj, I., and Pereira-Smith, O. (1995) A biomarker that identifies senescent human cells in culture and in aging skin *in vivo*. *Proc. Natl. Acad. Sci. U.S.A.* **92,** 9363–9367
31. Barsotti, A. M., and Prives, C. (2009) Pro-proliferative FoxM1 is a target of p53-mediated repression. *Oncogene* **28,** 4295–4305
32. Wang, I. C., Chen, Y. J., Hughes, D., Petrovic, V., Major, M. L., Park, H. J., Tan, Y., Ackerson, T., and Costa, R. H. (2005) Forkhead box M1 regulates the transcriptional network of genes essential for mitotic progression and genes encoding the SCF (Skp2-Cks1) ubiquitin ligase. *Mol. Cell. Biol.* **25,** 10875–10894
33. Wierstra, I., and Alves, J. (2007) FOXM1, a typical proliferation-associated transcription factor. *Biol. Chem.* **388,** 1257–1274
34. Abbas, T., and Dutta, A. (2009) p21 in cancer. Intricate networks and multiple activities. *Nat. Rev. Cancer* **9,** 400–414
35. Chen, Q., Fischer, A., Reagan, J. D., Yan, L. J., and Ames, B. N. (1995) Oxidative DNA damage and senescence of human diploid fibroblast cells. *Proc. Natl. Acad. Sci. U.S.A.* **92,** 4337–4341
36. Park, H. J., Carr, J. R., Wang, Z., Nogueira, V., Hay, N., Tyner, A. L., Lau, L. F., Costa, R. H., and Raychaudhuri, P. (2009) FoxM1, a critical regulator of oxidative stress during oncogenesis. *EMBO J.* **28,** 2908–2918
37. Halasi, M., and Gartel, A. L. (2009) A novel mode of FoxM1 regulation. Positive auto-regulatory loop. *Cell Cycle* **8,** 1966–1967
38. Chen, Y. J., Dominguez-Brauer, C., Wang, Z., Asara, J. M., Costa, R. H., Tyner, A. L., Lau, L. F., and Raychaudhuri, P. (2009) A conserved phosphorylation site within the forkhead domain of FoxM1B is required for its activation by cyclin-CDK1. *J. Biol. Chem.* **284,** 30695–30707
39. Alvarez-Fernández, M., Halim, V. A., Krenning, L., Aprelia, M., Mohammed, S., Heck, A. J., and Medema, R. H. (2010) Recovery from a DNA damage-induced G_2 arrest requires Cdk-dependent activation of FoxM1. *EMBO Rep.* **11,** 452–458